atmosphere

MDPI

Article

Determination of the Radon Progeny Activity Size Distribution in Laboratory Conditions

Eliska Fialova [1,2,*] and Petr P. S. Otahal [1]

[1] National Institute for Nuclear, Chemical and Biological Protection, 262 31 Milin, Czech Republic
[2] Department of Geological Sciences, Faculty of Science, Masaryk University, 602 00 Brno, Czech Republic
* Correspondence: fialovaeliska@sujchbo.cz; Tel.: +420-318-600-203

Abstract: Knowledge of the active size distribution of radon daughters is one of the main parameters for determining the effective dose from inhalation of short-term radon decay products. However, this parameter is crucial for accurately determining an effective dose; there are currently very limited possibilities for determining it. This paper describes the laboratory validation of a method for determining the activity size distribution of radon decay products using the Dekati ELPI+ cascade impactor and the Graded Screen Array Diffusion Battery (GSA DB). Using nuclear track detectors placed on individual impaction plates of the cascade impactor, the equivalent equilibrium activity concentration of individual size classes can be determined in the range from 17 nm to 10 µm. A diffusion battery was used to detect smaller particles in the unattached fraction area. The presented method can further refine the knowledge of the activity size distribution of radon decay products in different types of workplace atmospheres. Workplaces with higher radon concentrations differ significantly in the size distribution of aerosol particles, radon activity concentration, and equilibrium equivalent activity concentration.

Keywords: radon; radon daughter products; activity size distribution; radioactive aerosol

Citation: Fialova, E.; Otahal, P.P.S. Determination of the Radon Progeny Activity Size Distribution in Laboratory Conditions. *Atmosphere* **2024**, *15*, 1262. https://doi.org/10.3390/atmos15111262

Academic Editor: Chutima Kranrod

Received: 2 October 2024
Revised: 18 October 2024
Accepted: 20 October 2024
Published: 22 October 2024

1. Introduction

The inhalation of radon daughter products is one of the most significant contributors to the total effective dose from natural radioactive sources. The radon concentration at workplaces or in human dwellings varies significantly based on many parameters such as the geological background, indoor air exchange, building construction, and the year's season in which the measurement is carried out.

Effective doses from inhaled radon are determined mainly by the deposition of its alpha particle-emitting decay products on the epithelial lining of the respiratory tract. Deposition of the radioactive progeny depends on the aerosol characteristics. The equilibrium equivalent activity concentration (EEAC) is influenced, among other things, by the total concentration and size distribution of aerosol particles, relative humidity, and ventilation conditions. In addition to its activity concentration, the resulting effective dose from the inhalation of radon daughter products (RnDPs) is further influenced by the activity size distribution. Radon gas decays into solid short-lived radionuclides (Po-218, Pb-214, and Bi-214). The freshly formed radionuclides react rapidly (less than 1 s) with trace gases and vapours and grow by cluster formation to form particles around 1 nm in size. These are referred to as 'unattached progeny'. The unattached radionuclides may also attach to existing aerosol particles in the atmosphere within 1–100 s, forming the so-called 'attached progeny' [1].

Nearly the entire lung dose arises from the inhalation of the radon progeny aerosol and not from the gas itself. A large proportion of the inhaled radon progeny deposits in the respiratory tract of the lung, while almost all of the gas that is inhaled is subsequently exhaled. Due to the short half-lives of the radon progeny (less than 30 min), the dose is

delivered to the lung tissues before clearance can occur, either by absorption into the blood or particle transport to the alimentary tract. Two short-lived radon progeny (Po-218 and Po-214) decay by alpha emission and are predominant in the dose delivered to the lung tissues. Consequently, the lung dose accounts for more than 95% of the effective dose [2]. The hazard caused by inhalation of radon daughter products depends mainly on the site at which they pass through and deposit within the respiratory system. The fraction of the intake deposited in the respiratory tract primarily depends on the activity size distribution and physiological parameters such as breathing rate.

The ICRP 66 [3] describes the model used to calculate radiation doses delivered to the respiratory tract of workers resulting from the intake of airborne radionuclides. This dosimetric model considers the respiratory tract as four anatomic regions: extrathoracic, thoracic (bronchial), bronchiolar, and alveolar. The significant differences in radiation sensitivity among the respiratory tract tissues and the doses received from inhaled radionuclides argue for calculating radiation doses delivered to specific respiratory tract tissues.

The respiratory deposition occurs in a system of changing geometry with a flow that changes with time and cycles in direction. This means that different aerosol particles pass through various parts of the respiratory tract and cause different health risks. In general, due to their high mobility, the smallest particles in the area of an unattached fraction of radon decay products can pass through the whole respiratory tract into the alveolar part, deposit there, and cause much more significant radiation damage than attached radon daughter products.

This knowledge motivates the more extensive expansion of dosimetry requirements. The EEAC's size distribution is crucial for accurately estimating the radiation dose from inhaling radon decay products.

The activity size distribution can be determined over the whole size range of aerosol particles using a combination of a diffusion battery and a cascade impactor. The description of the basic functioning of the diffusion battery was presented in the articles of Knutson and Holub [4–6]. The use of a cascade impactor to determine the activity size distribution of radon daughter products is described, for example, by J. Kesten et al. [7]. Professor Solomon's team combined a diffusion battery and a cascade impactor to create the Radon Progeny Particle Size Spectrometer (RPPSS) instrument [8].

Measurement of the activity size distribution of radon daughter products using a diffusion battery has already been introduced and published by the SUJCHBO laboratories [9]. Therefore, the following works have focused on evaluating this unit using a cascade impactor combined with nuclear solid-state track detectors. This article presents the results of laboratory experiments with well-known radon and aerosol atmospheres.

2. Materials and Methods

2.1. Cascade Impactor

The electrical low-pressure impactor Dekati ELPI+ (Dekati Ltd., Kangasala, Finland) [10] was chosen to determine the activity size distribution. The cascade impactor is a real-time particle spectrometer for measuring airborne particle size distribution. The particles are first charged to a known charge level in a corona charger, and then, due to their aerodynamic diameter, they are classified in a low-pressure cascade impactor. The impactor stages are electrically insulated, and sensitive electrometers are connected to each impactor stage. The charged particles collected at a specific impactor stage produce an electrical current recorded by the respective electrometer channel. This current is proportional to the concentration of particles at each stage [11]. The ELPI+ impactor measures particles belonging to 14 size fractions in the range from 6 nm to 10 µm.

The 14 individual impactor stages operating in the range from 17 nm to 10 µm can be supplied by the collection substrate, which subsequently enables gravimetric or chemical analysis after the measurement. Before assembling the impactor, greased collection substrates must be inserted on the collection plates to prevent particles from bouncing during

the measurement. The final stage, which measures particles in the range from 6 to 17 nm, is a backup filter stage.

This device was operated in the cascade impactor mode without particle charging by a corona charger for the given purposes. In this mode, the cascade impactor works in the range from 17 nm up to 10 µm with fourteen deposition surfaces. The impactor operates at a nominal airflow of 10 L/min. Table 1 presents the sorting parameters of the cascade impactor.

Table 1. The sorting parameters of the Decati ELPI+ cascade impactor. $D_{50\%}$ mean particle diameter for 50% collection efficiency.

Deposition Surface	1	2	3	4	5	6	7	8	9	10	11	12	13	14
$D_{50\%}$ [µm]	0.017	0.03	0.06	0.108	0.17	0.26	0.4	0.64	1	1.6	2.5	4.4	6.8	10

2.2. Solid-State Nuclear Track Detector with Braking Foil

Equilibrium equivalent activity concentration (EEAC) is determined at each stage of the cascade impactor using the LR-115 solid-state nuclear track detector. This detection film is manufactured and supplied by Algade company (Algade, Bessines-sur-Gartempe, France), previously manufactured by KODAK (Eastman Kodak Company, Rochester, NY, USA). It is characterised by the energy discrimination of the detected alpha particle's energy in the 1 to 3 MeV range. For this reason, it is necessary to use a suitable braking foil to detect alpha particles with energies of more than 6 MeV that come from short-lived radon daughters. Based on calculations and tabulated values presented in ICRU 49 [12], a 50 µm thick Mylar foil was selected as the appropriate braking foil.

Before preparing a sampling set of all the cascade impactor´s deposition surfaces, the braking foil is treated with a collection substrate, preventing the sampled particles' recoil. Both foils, the threatened braking foil and the detection foil, are placed on the impact surface and fixed with a sealing sleeve. One disassembled and one assembled deposition plate of the cascade impactor are presented in Figures 1 and 2.

After the sampling, the detection foil is chemically processed, and a track density coming from the short-lived alpha particles of the radon decay products is determined on the whole surface of the detector using an optical microscope and automatic registration of traces. The track density at the particular deposition surface corresponds to EEAC. The background for each batch of detection film is determined and used for a more precise determination of EEAC.

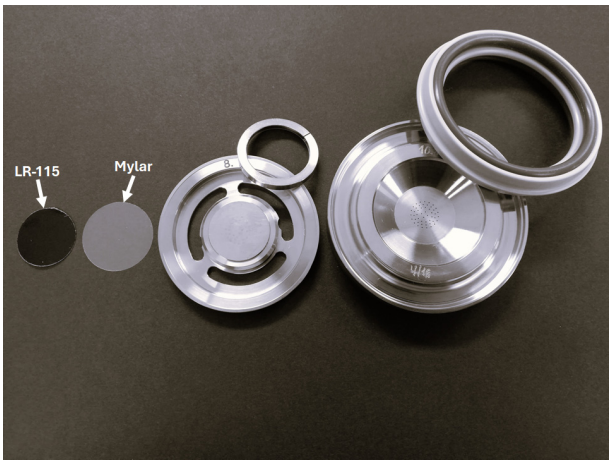

Figure 1. Disassembled deposition plate of the cascade impactor.

Figure 2. Assembled deposition plate of the cascade impactor.

The LR-115 detection foil has been used for many years in SUJCHBO laboratories to determine the long-term average of EEAC and the radon activity concentration. Its main applications are described in more detail in Chapter I. Burian of ref. [13].

2.3. Grab Sampling Method of f_p and EEAC Measurements

A fraction of progeny may not become attached to airborne particles, and this quantity is often referred to as the free or unattached fraction f_p. The unattached fraction is defined as the fraction of the potential alpha energy concentration of short-lived radon progeny that is not attached to the ambient aerosol [14].

EEAC is the concentration of Rn-222 in equilibrium with its progeny that would produce the same potential alpha energy concentration as the actual nonequilibrium mixture.

The grab sampling method uses the two-channel alpha spectrometer MAAF to determine EEAC and unattached fraction f_p. Two identical microfibre filters, AFPC (Merck SA, an affiliate of Merck KGaA, Darmstadt, Germany) or Sartorius Glasfibre Prefilter (Sartorius Corporation, Bohemia, NY, USA), are used for EEAC sampling and measurements. A diffusion screen (635 Mesh T316 Stainless.0008) and microfibre filter are used to measure f_p. In both methods, the air is sampled through the filters or the screen via sucking of the pump at a flow rate of 20 l/min and then measured simultaneously in the predefined time intervals after the end of sampling. Measured values are derived from these measurements [9].

The Authorised Metrological Centre and Calibration Laboratory of SUJCHBO uses the grab sampling methods. EEAC and f_p results are periodically compared to those of BfS Berlin with excellent results.

2.4. Diffusion Battery

The Graded Screen Array Diffusion Battery (GSA DB) was used to determine the activity size distribution of radon daughter products in the 0.3 to 100 nm range. The device consists of 10 graded diffusion screens and a backup filter. After sampling ends, the graded screens' alpha activity and filter are measured using the two-channel alpha activity meter MAAF [9].

2.5. Scanning Mobility Particle Sizer Spectrometer

The SMPS 3938 (Scanning Mobility Particle Sizer Spectrometer, TSI Incorporated, Shoreview, MN, USA) was used to determine the size distribution of aerosol particles. This aerosol spectrometer divides the determined size distribution into 192 size classes in a measuring range from 1 nm to 1 µm. The minimum sampling interval length is 15 s [15].

The comparison of the activity size distribution determined using the Dekati ELPI+ cascade impactor and the numerical size distribution determined using the SMPS 3938 is made based on comparing the geometric mean of the particle size. The geometric mean is

defined in size ranges in which both instruments are sampled and calculated based on the following relationship:

$$\bar{x}_g = e^{\left(\frac{\sum_l^u n \ ln \ D_p}{N}\right)} \quad (1)$$

where:

$\bar{x}_g$—geometric mean;
n—number weighted concentration per size channel;
D_p—particle diameter (channel midpoint);
l—lower size channel boundary;
u—upper size channel boundary;
N—total number concentration/track density.

2.6. Aerosol Sources

The AGK-2000 generator (Palas, Germany) with an aqueous NaCl solution was used as a source of aerosol particles. Cigarette smoke was used to generate different types of aerosols and compare results. Both aerosol sources were chosen based on the various densities of generated particles. The density of NaCl is 2.16 g/cm^3, and the density of cigarette smoke is 1.18 g/cm^3 [16]. For a better results comparison, the mobility diameter of aerosol particles determined by SMPS was converted to the aerodynamic diameter determined by Dekati ELPI+. The dependence between the compared diameter and the density of measured particles was used for the recalculation according to Baron and Willeke [17]:

$$d_a = d_m \left(\frac{\rho_p}{\rho_0}\right)^{1/2} \quad (2)$$

where:

d_a—aerodynamic diameter;
d_m—mobility diameter;
ρ_p—density of the aerosol particle;
ρ_0—density of standardized particle (1 g/cm^3).

3. Experimental Section

The experiments were carried out in the laboratory of the Nuclear Protection Department, which is part of SUJCHBO. This laboratory contains a unique Testing Room equipped with a separate source of radon dotted into the room from the bedrock. In addition, the testing room is equipped with a special ventilation system, which enables a controlled exchange of inside air. Aerosol filters placed in the ventilation system's branches prevent indoor atmosphere contamination by outdoor aerosols. Radioactive aerosols were always sampled at least three hours after cleaning the indoor atmosphere from the previous aerosol, injecting a new aerosol, and establishing the equilibrium of radon and its daughter products. To ensure the relative homogeneity of the sampled aerosols, the samplings were carried out in the middle of the testing room to avoid the influence of the boundary layer at the walls.

Different radon and aerosol atmospheres were prepared in the testing room to verify the methodology for determining the activity size distribution of radon decay products.

To ensure the possibility of comparing the total equilibrium equivalent activity concentration (EEAC) with the results of the EEAC determined across the individual stages of the cascade impactor and the diffusion battery (activity size distribution), the EEAC and f_p were determined using grab sampling methods. All samples were always tested at the same time. The time integral of EEAC [Bq·h·m^{-3}] was calculated from the results of EEAC obtained by the grab sampling method. The total time integral corresponds to the sampling time of radon daughter products (RnDPs) using the cascade impactor and the diffusion battery. During the experiments in the laboratory conditions, the sampling time was chosen based on the EEAC level, which ranged from 5 to 20 min. For the grab

sampling method, 20 min is the maximal sampling time due to the accredited methodology of the Authorised Metrological Centre.

4. Results and Discussion

4.1. Choosing an Appropriate Braking Foil

A series of tests of various commercially available braking foils was carried out according to the determined decrease in the energy of the alpha particles depending on the area weight specified in ICRU 49 [12]. Based on the results of the experiments, two types of Mylar foils with thicknesses of 50 µm and 36 µm were selected. The initial experiments aimed to determine the suitability of the foil used and the saturation area. The experiments were carried out in different EEAC conditions ranging from 700 to 12,500 Bq·h·m^{-3}. Based on these results, the foil with a thickness of 50 µm was selected as the most appropriate foil. A summary of the initial experiments is presented in Figure 3.

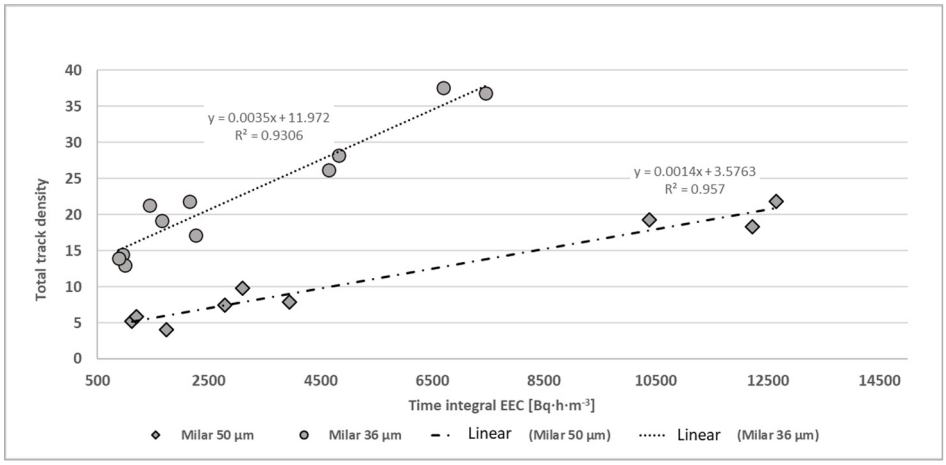

Figure 3. Determination of the saturation for selected types of braking foils.

The individual points in the graph on the y-axis present the sum of the track density from all impactor plates (the total track density). On the x-axis, individual time integrals measured during experiments by the grab sampling methods are presented. In the case of Mylar 36, more tracks were detected, so the determination of EEAC was more precise. On the other hand, the detection foil could be saturated much earlier, at about 200 Bq·h·m^{-3}. Based on the more suitable parameters of the regression line, which indicate a more extensive range of use and later saturation of the detector at a higher time integral, a 50 µm thick Mylar braking foil was selected. At a time integral above 2.5 kBq·h·m^{-3}, the traces merge, and the saturation becomes evident. The overexposed track detectors could not be evaluated. For this reason, further experiments were carried out below this limit of the time integral.

4.2. Relationship Between EEAC and Track Density

Figure 4 summarizes experiments establishing the relationship between the time integral of the EEAC and the total track density. The graph in Figure 4 presents a good agreement between the total track density and the time integral of the EEAC determined by the grab sampling method used in the Authorized Metrological Center. The y-axis presents the sum of track density from all stages of the cascade impactor after the average detector background was subtracted. The dispersion of results could be caused by the uncertainty of the flow rate, detectors' background, or sampling time. The time integral of the EEAC used for laboratory experiments ranged from 50 to 2000 Bq·h·m^{-3}.

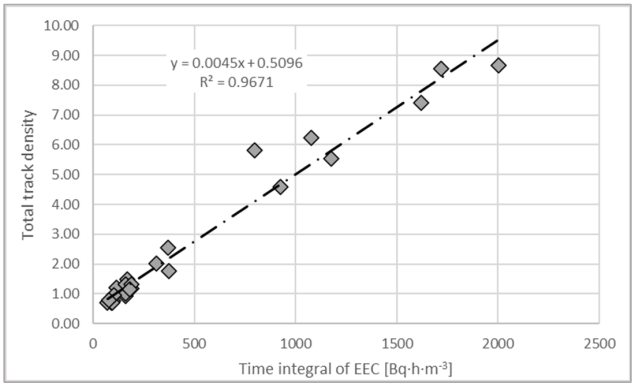

Figure 4. Relationship between the time integral of EEAC and the total track density.

4.3. Comparison of the Activity Size Distribution and the Size Distribution

Further experiments aimed to compare the EEAC size distribution determined by the cascade impactor and the size distribution determined using the SMPS. These experiments were carried out with two types of aerosol particles (cigarette smoke and NaCl). The different densities of the generated aerosol manifest themselves by shifting in the size distribution. In the case of the cigarette smoke aerosol, which has a density of 1.18 g/cm^3, the shift in size is not so significant. The shift of the mobility diameter to the aerodynamic diameter is far more pronounced in the case of the NaCl aerosol, which has a density of 2.16 g/cm^3. The results of the recalculation for the NaCl aerosol are demonstrated in Figure 5. The primary size mode presented in Figure 5 changes from 117.6 nm to 172.8 nm when converted from mobility to aerodynamic diameter using Equation (2). Figure 5 describes changes in the size distribution of a general aerosol (nonradioactive) measured by the SMPS for comparison with the results of size distribution determined by the cascade impactor. During comparison experiments with the SMPS, such aerosol concentrations and size distributions were generated to suppress coagulation as much as possible, which would potentially lead to a change in the main size mode. Moreover, samplings by the cascade impactor were always carried out after the stabilization of the atmosphere, which consisted of a precise mixing of generated aerosol in the testing room. The spectrums from the SMPS that were compared present the mean value of the size distribution gained from many measurements that were collected during sampling by the cascade impactor.

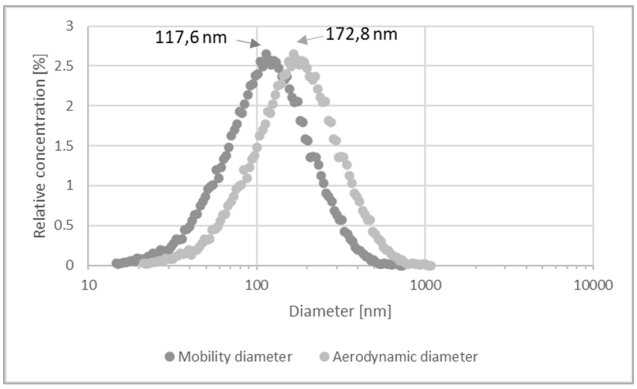

Figure 5. The recalculation of the mobility diameter to the aerodynamic diameter for NaCl aerosol.

For both comparisons demonstrated in Figures 6 and 7, the size distribution was converted to the aerodynamic diameter, which is used on the x-axis. In Figure 6, the primary size mode measured by the SMPS is 219 nm for the aerosol generated from cigarette smoke. In Figure 7, the primary size mode measured by the SMPS is 166 nm for the aerosol generated from the NaCl solution.

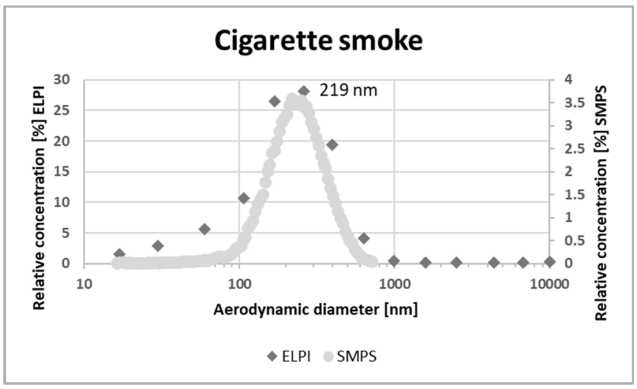

Figure 6. Comparison of aerosol generated by cigarette smoke.

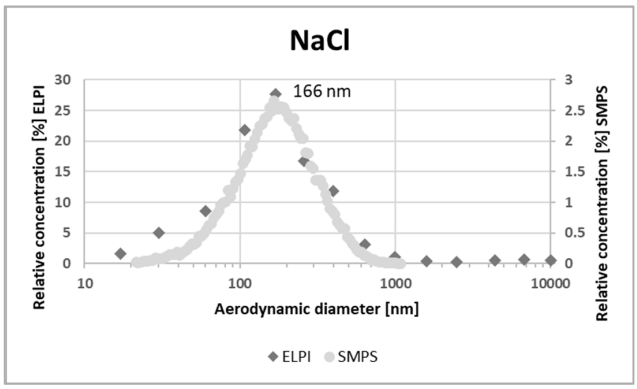

Figure 7. Comparison of aerosol generated by NaCl.

Table 2 presents the calculated geometric averages of aerosols from the individual size ranges from 10 nm to 1 µm.

Table 2. Calculated geometrical averages of aerosols.

Source of Aerosol	SMPS [nm]	ELPI [nm]
NaCl	166	156
Cigarette smoke	230	198

The agreement between the geometric diameter determined using the SMPS and the ELPI+ cascade impactor is mainly influenced by the number and width of the individual size channels.

4.4. Determination of Activity Size Distribution in the Unattached Fraction Area

As mentioned, the activity size distribution from 17 nm to 10 µm can be determined using the ELPI+ cascade impactor. The diffusion battery was added to the methodology to ensure the possibility of determining the whole activity size distribution, including the unattached fraction area. Figure 8 shows the measured activity size distribution using the ELPI+ cascade impactor and the diffusion battery under laboratory conditions with an f_p of 0.77 and an EEAC of 412 Bq·m^{-3}. Both values (f_p and EEAC) were measured simultaneously using the grab sampling methods. The air was sampled by the diffusion battery and cascade impactor at the same time in the prepared atmosphere of the testing room. The sum of EEAC determined with the help of the diffusion battery and the cascade impactor through all size modes is 440 Bq·m^{-3}. A good agreement between the results obtained with the help of grab sampling methods and the results obtained by the cascade impactor and the diffusion battery enables a determination of the whole activity size distribution of radon daughter products, including the free fraction.

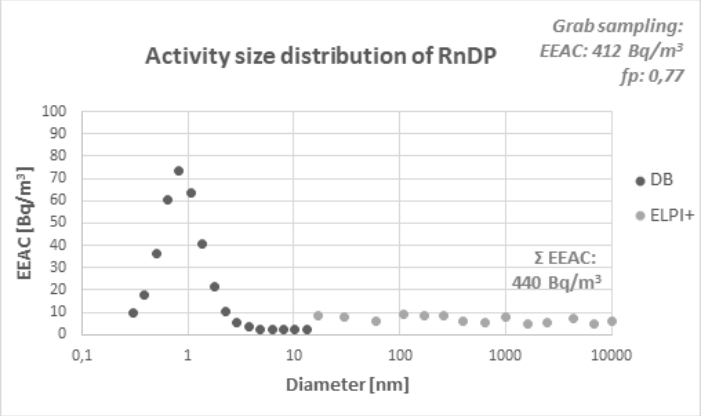

Figure 8. Activity size distribution of RnDP determined by the cascade impactor (ELPI+) and the diffusion battery (DB).

Figures 9 and 10 show the correlation between the unattached fraction f_p and the EEAC compared to the values determined by the grab sampling methods used in the Calibration Laboratory SUJCHBO. All samples were tested in conditions with a high f_p that ranged from 0.63 to 0.83.

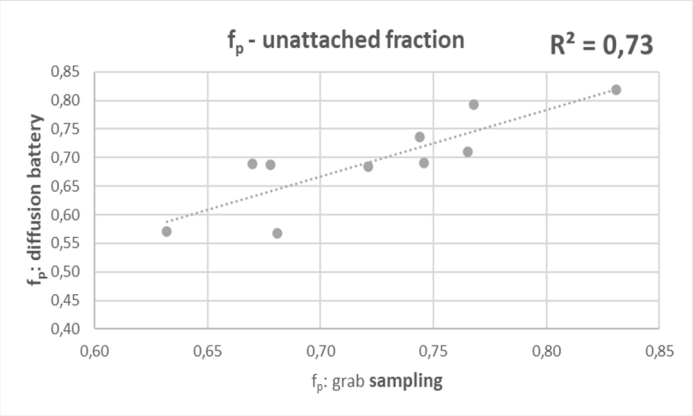

Figure 9. Correlation of f_p determined by the diffusion battery compared to the grab sampling method.

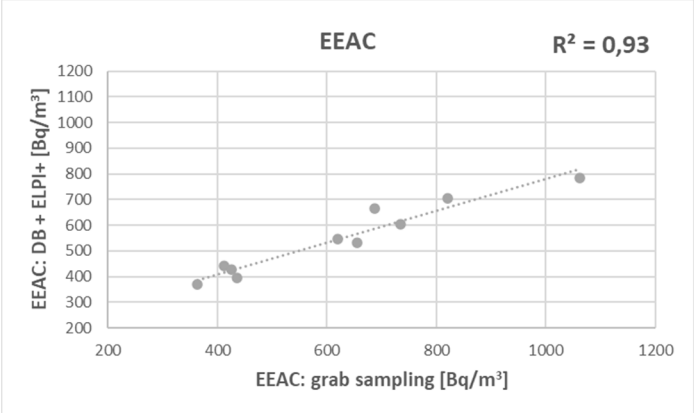

Figure 10. Correlation of EEAC determined simultaneously by the cascade impactor (ELPI+) and the diffusion battery (DB) compared to the grab sampling method.

5. Conclusions

Laboratory experiments verified the suitability of determining the activity size distribution using the Dekati ELPI+ cascade impactor. Each stage of this cascade impactor is fitted with an LR-115 detection film and a 50 μm thick Mylar braking foil. The calibration dependence between the total track density and the time integral of the equilibrium equivalent activity concentration was determined using laboratory experiments that were conducted in a well-known radon and aerosol atmosphere. Furthermore, the working measurement range corresponding to a maximum of 2.5 kBq·h·m^{-3} was determined during the laboratory measurements. At a time integral above 2.5 kBq·h·m^{-3}, the traces were already merging, and thus, the determined track density became less accurate or could not be evaluated at all. To use the methodology in the field, it is necessary to know the EEAC and adjust (decrease) the sampling time to avoid the overexposure of the solid-state detectors. On the other hand, under very low EEAC conditions, the dispersion of the track density was extremely high and caused increasing uncertainty. In this case, it is necessary to increase the sampling time. The correctness of the developed method was verified by comparing it with the number size distribution determined using the SMPS. Knowing the density of the generated aerosol allows for comparing the aerodynamic and mobility diameters. Knowing the density of the sampled aerosol is necessary for comparing the individual size distributions of different aerosol measurement methods.

The diffusion battery system must supplement the measuring method in specific radon and aerosol atmospheres with high unattached fractions. After that, using the ELPI+ cascade impactor with solid-state nuclear track detectors combined with the diffusion battery enables the determination of the activity size distribution of radon daughter products in the whole aerosol size spectrum in the area of the attached fraction as well as in the area of the unattached fraction.

Future measurements will be carried out at selected workplaces in the following period, assuming various equilibrium equivalent activity concentration values. The sampling time has to be settled and adopted based on the supposed or measured EEAC to avoid the overexposure of the solid-state nuclear track detectors. The presented method can refine the knowledge of the activity size distribution of radon decay products in different workplace atmospheres and make dosimetry requirements much more accurate. The calculation of conversion coefficients for the effective dose from the inhalation of radon daughter products can be precise using this method.

Author Contributions: Conceptualization, E.F. and P.P.S.O.; methodology, P.P.S.O.; software, P.P.S.O.; validation, E.F. and P.P.S.O.; formal analysis, E.F. and P.P.S.O.; investigation, E.F. and P.P.S.O.; resources, E.F. and P.P.S.O.; data curation, E.F. and P.P.S.O.; writing—original draft preparation, E.F. and P.P.S.O.; writing—review and editing, E.F. and P.P.S.O.; visualization, E.F. and P.P.S.O.; supervision, P.P.S.O.; project administration, P.P.S.O.; funding acquisition, E.F. and P.P.S.O. All authors have read and agreed to the published version of the manuscript.

Funding: This research was funded by the Euratom Research and Training Programme 2019–2020 under grant number 900009. It was also funded with the institutional support of Masaryk University Brno.

Institutional Review Board Statement: Not applicable.

Informed Consent Statement: Not applicable.

Data Availability Statement: The datasets presented in this article are not readily available because the data are part of an ongoing study. Requests to access the datasets should be directed to the corresponding author.

Acknowledgments: Many thanks to Robert Holub for spearheading the development of the method.

Conflicts of Interest: The authors declare no conflicts of interest.

References

1. Porstendörfer, J. Physical parameters and dose factors of the radon and thoron decay products. *Radiat. Prot. Dosim.* **2001**, *94*, 365–373. [CrossRef] [PubMed]
2. Harrison, J.D.; Marsh, J.W. Effective dose from inhaled radon and its progeny. *Ann. ICRP* **2012**, *41*, 378–388. [CrossRef] [PubMed]
3. ICRP. Human respiratory tract model for radiological protection. ICRP Publication 66. *Ann. ICRP* **1994**, *24*, 1–3.
4. Holub, R.F.; Knutson, E.O. Measurement of 218Po diffusion coefficient spectra using multiple wire screens. *ACS Symp. Ser.* **1987**, *331*, 340–356; Radon and its decay products. [CrossRef]
5. Knutson, E.O.; George, A.C.; Wu, T.K. The graded screen technique for measuring the diffusion coefficient of radon decay products. *Aerosol Sci. Technol.* **1997**, *27*, 604–624. [CrossRef]
6. Knutson, E.O. History of Diffusion Batteries in Aerosol Measurements. *Aerosol Sci. Technol.* **1999**, *31*, 83–128. [CrossRef]
7. Kesten, J.; Porstendörfer, J.; Butterweck, G.; Reineking, A.; Heymel, H.J. An online α-Impactor for Short-Lived Radon Daughters. *Aerosol Sci. Technol.* **1993**, *18*, 156–164. [CrossRef]
8. Solomon, S.B. *Manual for Radon Progeny Particle Size Spectrometer (RPPSS)*; ARPANSA: Yallambie, Australia, 1999.
9. Otahal, P.P.S.; Burian, I.; Ondracek, J.; Zdimal, V.; Holub, R.F. Simultaneous measurements of nanoaerosols and radioactive aerosols containing the short-lived radon isotopes. *Radiat. Prot. Dosim.* **2017**, *177*, 53–56. [CrossRef] [PubMed]
10. Keskinen, J.; Pietarinen, K.; Lehtimaki, M. Electric Low-Pressure Impactor. *J. Aerosol Sci.* **1992**, *23*, 353–360. [CrossRef]
11. Dekati. *ELPI+ User Manual Version 1.22*; Dekati: Tykkitie, Finland, 2014.
12. ICRU. *Stopping Powers and Ranges for Protons and Alpha Particles, 1993, Report No. 49*; International Commission on Radiation Units: Bethesda, MD, USA, 1993.
13. Sidorov, M.; Ivanov, O. *Chapter: Use of SSNTD in the Czech Republic (Burian, I.) in Nuclear Track Detectors—Design, Methods and Applications*; Nova Science Publisher Inc.: New York, NY, USA, 2010; pp. 241–252. ISBN 9781608768264.
14. ICRU. Measurement and Reporting of Radon Exposures, 1995, Report No. 88. In *Journal of the ICRU*; Oxford University Press: New York, NY, USA, 2012; Volume 12. [CrossRef]
15. TSI. *Electrostatic Classifier Model 3082, SMPS 3938, Operation and Service Manual, 2020, P/N 6006760, Revision D*; TSI: Buckinghamshire, UK, 2016.
16. Johnson, T.J.; Olfert, J.S.; Cabot, R.; Treacy, C.; Yurteri, C.U.; Dickens, C.; McAughey, J.; Symonds, J.P.R. Steady-state measurement of the effective particle density of cigarette smoke. *J. Aerosol Sci.* **2014**, *75*, 9–16. [CrossRef]
17. Baron, P.A.; Willeke, K. *Aerosol Measurement: Principles, Techniques, and Applications*; Wiley: New York, NY, USA, 2011; p. 51. ISBN 978-0-470-38741-2.